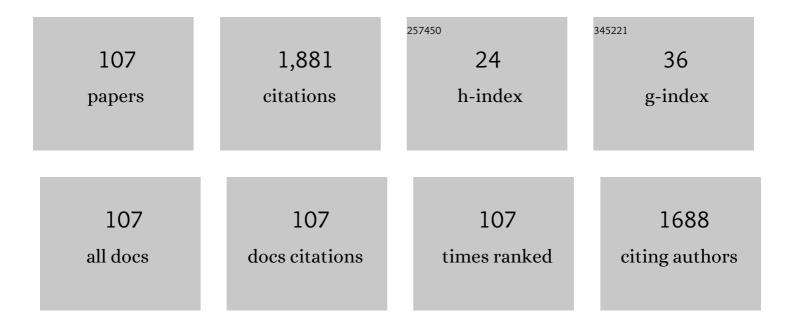
List of Publications by Year in descending order

Source: https://exaly.com/author-pdf/7259413/publications.pdf Version: 2024-02-01



#	Article	IF	CITATIONS
1	Fluorine substituted thiophene–quinoxalinecopolymer to reduce the HOMO level and increase the dielectric constant for high open-circuit voltage organic solar cells. Journal of Materials Chemistry C, 2013, 1, 630-637.	5.5	101
2	N-doped carbon nanocages: Bifunctional electrocatalysts for the oxygen reduction and evolution reactions. Nano Research, 2018, 11, 1905-1916.	10.4	73
3	N,F-Codoped Carbon Nanocages: An Efficient Electrocatalyst for Hydrogen Peroxide Electroproduction in Alkaline and Acidic Solutions. ACS Sustainable Chemistry and Engineering, 2020, 8, 2883-2891.	6.7	72
4	Lateral substituent effects on UV stability of high-birefringence liquid crystals with the diaryl-diacetylene core: DFT/TD-DFT study. Liquid Crystals, 2017, 44, 1515-1524.	2.2	56
5	Multistimuliâ€Responsive Selfâ€Organized Liquid Crystal Bragg Gratings. Advanced Optical Materials, 2019, 7, 1900101.	7.3	56
6	Cyclic Thiourea/Urea Functionalized Triphenylamine-Based Dyes for High-Performance Dye-Sensitized Solar Cells. Organic Letters, 2013, 15, 1456-1459.	4.6	55
7	Dielectric and optical anisotropy enhanced by 1,3-dioxolane terminal substitution on tolane-liquid crystals. Journal of Materials Chemistry C, 2015, 3, 8706-8711.	5.5	48
8	Highly Active Hollow RhCu Nanoboxes toward Ethylene Glycol Electrooxidation. Small, 2021, 17, e2006534.	10.0	48
9	Block poly(arylene ether sulfone) copolymers tethering aromatic side-chain quaternary ammonium as anion exchange membranes. Polymer Chemistry, 2018, 9, 699-711.	3.9	46
10	Facile synthesis and the properties of novel cardo poly(arylene ether sulfone)s with pendent cycloaminium side chains as anion exchange membranes. Polymer Chemistry, 2017, 8, 4207-4219.	3.9	45
11	Grapheneâ€Encapsulated Co <sub>9</sub> S <sub>8</sub> Nanoparticles on N,Sâ€Codoped Carbon Nanotubes: An Efficient Bifunctional Oxygen Electrocatalyst. ChemSusChem, 2019, 12, 3390-3400.	6.8	43
12	High performance liquid crystals for vehicle displays. Optical Materials Express, 2016, 6, 717.	3.0	40
13	Fe/N Codoped Carbon Nanocages with Single-Atom Feature as Efficient Oxygen Reduction Reaction Electrocatalyst. ACS Applied Energy Materials, 2018, 1, 4982-4990.	5.1	38
14	Improved nematic mesophase stability of benzoxazole-liquid crystals via modification of inter-ring twist angle of biphenyl unit. Liquid Crystals, 2016, 43, 1397-1407.	2.2	36
15	In situ conversion of iron sulfide (FeS) to iron oxyhydroxide (γ-FeOOH) on N, S co-doped porous carbon nanosheets: An efficient electrocatalyst for the oxygen reduction reaction and zinc–air batteries. Journal of Colloid and Interface Science, 2020, 558, 323-333.	9.4	34
16	Synthesis and properties of substituted benzoxazole-terminated liquid crystals. Liquid Crystals, 2013, 40, 197-215.	2.2	33
17	Improving UV stability of tolane-liquid crystals in photonic applications by the ortho fluorine substitution. Optical Materials Express, 2016, 6, 97.	3.0	33
18	Low mid-infrared absorption tolane liquid crystals terminated by 2,2-difluorovinyloxyl: synthesis, characterization and properties, Journal of Materials Chemistry C. 2016, 4, 4939-4945.	5.5	32

ZHONGWEI AN

#	Article	IF	CITATIONS
19	Tolane liquid crystals bearing fluorinated terminal group and their mid-wave infrared properties. Liquid Crystals, 2014, 41, 1696-1702.	2.2	30
20	Co-sensitization of N719 with an Organic Dye for Dye-sensitized Solar Cells Application. Bulletin of the Korean Chemical Society, 2014, 35, 1449-1454.	1.9	30
21	The effect of lateral fluorination on the properties of phenyl-tolane liquid crystals. Liquid Crystals, 2015, 42, 397-403.	2.2	28
22	0.2 V Electrolysis Voltage-Driven Alkaline Hydrogen Production with Nitrogen-Doped Carbon Nanobowl-Supported Ultrafine Rh Nanoparticles of 1.4 nm. ACS Applied Materials & Interfaces, 2019, 11, 35039-35049.	8.0	27
23	Approach to tune short-circuit current and open-circuit voltage of dye-sensitized solar cells: π-linker modification and photoanode selection. RSC Advances, 2014, 4, 42252-42259.	3.6	26
24	Highly fluorinated liquid crystals with wide nematic phase interval and good solubility. Liquid Crystals, 2014, 41, 1783-1790.	2.2	25
25	Cyclic thiourea functionalized dyes with binary π-linkers: Influence of different π-conjugation segments on the performance of dye-sensitized solar cells. Dyes and Pigments, 2015, 116, 146-154.	3.7	25
26	Synthesis and mesomorphic properties of 7-alkoxybezopyrano[2,3-c]pyrazol-3-one. Liquid Crystals, 2010, 37, 1549-1557.	2.2	24
27	Synthesis and mesomorphic properties of 2-(4′-alkoxybiphenyl-4-yl)-1 <i>H</i> -benzimidazole derivatives. Liquid Crystals, 2013, 40, 396-410.	2.2	24
28	Nematic mesophase enhanced via lateral monofluorine substitution on benzoxazole-liquid crystals. Liquid Crystals, 2016, 43, 1341-1350.	2.2	24
29	Benzoxazole-terminated liquid crystals with high birefringence and large dielectric anisotropy. Liquid Crystals, 2020, 47, 1274-1280.	2.2	24
30	Synthesis and mesomorphic properties of but-3-enyl-based fluorinated biphenyl liquid crystals. Liquid Crystals, 2012, 39, 457-465.	2.2	23
31	Synthesis and properties of allyloxy-based tolane liquid crystals with high negative dielectric anisotropy. Liquid Crystals, 2017, 44, 2184-2191.	2.2	23
32	Synthesis and characterisation of benzoxazole-based liquid crystals possessing 3,5-difluorophenyl unit. Liquid Crystals, 2014, 41, 1455-1464.	2.2	20
33	Synthesis, mesomorphic and gelation properties of 7-alkoxycoumarin-3-carbonyl hydrazine. Liquid Crystals, 2012, 39, 1393-1401.	2.2	19
34	New isothiocyanato liquid crystals containing thieno[3,2- <i>b</i> ]thiophene central core. Liquid Crystals, 2018, 45, 1294-1302.	2.2	19
35	Synthesis and properties of mesogenic laterally fluorinated compounds containing benzoxazole unit. Liquid Crystals, 2014, 41, 1042-1056.	2.2	18
36	Synthesis and physical properties of tolane liquid crystals containing 2,3-difluorophenylene and terminated by a tetrahydropyran moiety. Liquid Crystals, 2016, 43, 564-572.	2.2	18

#	Article	IF	CITATIONS
37	The effect of locations of triple bond at terphenyl skeleton on the properties of isothiocyanate liquid crystals, 2017, 44, 1374-1383.	2.2	18
38	High electrocapacitive performance of bowl-like monodispersed porous carbon nanoparticles prepared with an interfacial self-assembly process. Journal of Colloid and Interface Science, 2017, 496, 35-43.	9.4	18
39	High-frame-rate liquid crystal phase modulator for augmented reality displays. Liquid Crystals, 2019, 46, 309-315.	2.2	18
40	Synthesis and mesomorphic properties of benzoxazole derivatives with lateral multifluoro substituents. Liquid Crystals, 2019, 46, 59-66.	2.2	17
41	Synthesis and evaluation of simple molecule as a co-adsorbent dye for highly efficient co-sensitized solar cells. Dyes and Pigments, 2015, 120, 85-92.	3.7	16
42	Preparation and characterisation of laterally monofluorinated mesogenic benzimidazole-based compounds. Liquid Crystals, 2017, 44, 1678-1685.	2.2	15
43	Synthesis and study the liquid crystalline properties of compounds containing benzoxazole core and terminal vinyl group. Liquid Crystals, 2019, 46, 797-805.	2.2	15
44	Synthesis and mesomorphic properties of the nematic mesophase benzoxazole derivatives with big twist angle of difluoro-biphenyl unit. Liquid Crystals, 2019, 46, 1013-1023.	2.2	15
45	The effect of furan linkers on the properties of cyclic thiourea functionalized triphenylamine dye sensitizers. Dyes and Pigments, 2017, 139, 772-778.	3.7	13
46	New isothiocyanatotolane liquid crystals with terminal but-3-enyl substitute. Liquid Crystals, 2017, 44, 833-842.	2.2	13
47	Investigation of terminal olefine in the isothiocyanatotolane liquid crystals with alkoxy end group. Liquid Crystals, 2018, 45, 1498-1507.	2.2	13
48	Investigation of 4-pyridyl liquid crystals on the photovoltaic performance and stability of dye sensitized solar cells by the co-sensitization. Dyes and Pigments, 2018, 159, 527-532.	3.7	13
49	Effect of the Spatial Configuration of Donors on the Photovoltaic Performance of Double Dâ~'π–A Organic Dyes. ACS Applied Materials & Interfaces, 2021, 13, 40648-40655.	8.0	13
50	Covalently and ionically crosslinked sulfonated poly(arylene ether ketone)s as proton exchange membranes. Polymer Bulletin, 2012, 68, 1369-1386.	3.3	12
51	Preparation and properties of laterally multifluorinated benzoxazole-based nematic mesogens. Liquid Crystals, 2017, 44, 1686-1694.	2.2	12
52	The effect of intermolecular actions on the nematic phase range of tolane-liquid crystals. Liquid Crystals, 2018, 45, 783-792.	2.2	12
53	The effect of phenyl ring on the physical properties of liquid crystals containing 4-pyridyl terminal group. Liquid Crystals, 2018, 45, 1825-1833.	2.2	12
54	Dissecting terminal fluorinated regulator of liquid crystals for fine-tuning intermolecular interaction and molecular configuration. Journal of Molecular Liquids, 2020, 310, 113225.	4.9	12

ZHONGWEI AN

#	Article	IF	CITATIONS
55	Synthesis and properties of 5,6-dihydro-4H-cyclopenta[b]thiophene-based nematic liquid crystals: A new access to mesogens with high birefringence and large dielectric anisotropy. Journal of Molecular Liquids, 2021, 327, 114827.	4.9	12
56	Synthesis and properties of allyloxy-based biphenyl liquid crystals with multiple lateral fluoro substituents. Liquid Crystals, 2012, 39, 957-963.	2.2	11
57	Highly Efficient Dyeâ€sensitized Solar Cells by Coâ€sensitization of Organic Dyes and Coâ€adsorbent Chenodeoxycholic Acid. Chinese Journal of Chemistry, 2014, 32, 474-478.	4.9	10
58	The effect of terminal epoxy modification on the mesomorphic and thermal stability of biphenyl ester liquid crystals. Liquid Crystals, 2019, 46, 2149-2158.	2.2	10
59	Unclogging electron-transporting channels via self-assembly for improving light harvesting and stability of dye-sensitized solar cells. Electrochimica Acta, 2019, 299, 518-530.	5.2	10
60	5,6-Difluorobenzofuran: a new core for the design of liquid crystal compound with large dielectric anisotropy and broad nematic range. Liquid Crystals, 2021, 48, 273-280.	2.2	10
61	Effect of <i>ï€-</i> conjugation units on the liquid crystal and photovoltaic performance of heterocyclic pyridine-based compounds. Liquid Crystals, 2021, 48, 2178-2187.	2.2	10
62	Acid@base co-sensitization strategy for highly efficient dye-sensitized solar cells. Optical Materials, 2021, 121, 111528.	3.6	10
63	Improved mesomorphic behaviour and large birefringence of fluorinated liquid crystals containing ethynyl and 1-methyl- <i>1H</i> -benzimidazole moieties. Liquid Crystals, 2020, 47, 1264-1273.	2.2	9
64	Low dielectric loss and good miscibility of the tolane liquid crystals by tuning their lateral substituents. Journal of Molecular Liquids, 2021, 325, 115236.	4.9	9
65	Synthesis and properties of benzoxazole-terminated mesogenic compounds containing tolane with high birefringence and large dielectric anisotropy. Liquid Crystals, 2021, 48, 1978-1991.	2.2	9
66	Imidazole-Functionalized Multiquaternary Side-Chain Polyethersulfone Anion-Exchange Membrane for Fuel Cell Applications. ACS Applied Energy Materials, 2022, 5, 10023-10033.	5.1	9
67	Covalentâ€ionically crosslinked sulfonated poly(arylene ether sulfone)s bearing quinoxaline crosslinkages as proton exchange membranes. Journal of Applied Polymer Science, 2012, 124, E278.	2.6	8
68	New Mesogenic Compounds Containing a Terminal-Substituted Benzoxazole Unit. Molecular Crystals and Liquid Crystals, 2014, 592, 44-62.	0.9	8
69	Poly(arylene ether sulfone) bearing multiple benzyl-type quaternary ammonium pendants: preparation, stability and conductivity. RSC Advances, 2017, 7, 30770-30783.	3.6	8
70	Interface self-assembly preparation of multi-element doped carbon nanobowls with high electrocatalysis activity for oxygen reduction reaction. Journal of Colloid and Interface Science, 2019, 533, 569-577.	9.4	8
71	Effect of Extending the Conjugation of Dye Molecules on the Efficiency and Stability of Dye-Sensitized Solar Cells. ACS Omega, 2021, 6, 30069-30077.	3.5	8
72	New terphenyl liquid crystals terminated by 2-chloro-3,3,3-trifluoropropenyl group. Liquid Crystals, 2017, 44, 1646-1652.	2.2	7

#	Article	IF	CITATIONS
73	Study on dye-loading mode on TiO2 films and impact of co-sensitizers on highly efficient co-sensitized solar cells. Journal of Materials Science: Materials in Electronics, 2017, 28, 3962-3969.	2.2	7
74	The effect of intermolecular actions on the mesomorphic properties of alkenoxy biphenyl-based liquid crystals. Journal of Molecular Liquids, 2019, 296, 111880.	4.9	7
75	Preparation and properties of 1-methyl- <i>1H</i> -benzimidazole-based mesogenic compounds incorporating ethynyl moiety. Liquid Crystals, 2020, 47, 1281-1290.	2.2	7
76	New block poly(ether sulfone) based anion exchange membranes with rigid side-chains and high-density quaternary ammonium groups for fuel cell application. Polymer Chemistry, 2022, 13, 4395-4405.	3.9	7
77	Synthesis and properties of benzoxazole-based liquid crystals containing ethynyl group. Liquid Crystals, 2020, 47, 1719-1728.	2.2	6
78	Mesomorphic properties improved via lateral fluorine substituent on benzoxazole-terminated mesogenic compounds. Liquid Crystals, 2020, 47, 1555-1568.	2.2	6
79	Benzoxazole-based nematic liquid crystals containing ethynyl and two lateral fluorine atoms with large birefringence. Liquid Crystals, 2021, 48, 157-167.	2.2	6
80	Quinoxaline-based semi-interpenetrating polymer network of sulfonated poly(arylene ether)s and sulfonated polyimides as proton exchange membranes. Polymer Bulletin, 2021, 78, 4333-4354.	3.3	6
81	Introduction of 5,6-dihydro-4 <i>H</i> -cyclopenta[ <i>b</i> ]thiophene core unit into phenyl-tolane: Expanding the mesophase range and increasing the birefringence and dielectric anisotropy of liquid crystal. Liquid Crystals, 2021, 48, 1650-1659.	2.2	6
82	The effect of benzoxazole unit on the properties of cyclic thiourea functionalized triphenylamine dye sensitizers. Dyes and Pigments, 2021, 187, 109093.	3.7	6
83	Synthesis and properties of difluoromethyleneoxy-bridged liquid crystals terminated by 2,2-difluorovinyloxy group. Liquid Crystals, 2015, 42, 383-389.	2.2	5
84	The effect of cyclic thiourea functionalization and β,β′-dialkylbithiophene linker on the performance of triphenylamine dyes. Journal of Molecular Structure, 2015, 1094, 195-202.	3.6	5
85	Preparation and mesomorphic properties of 1-methyl- <i>1H</i> -benzimidazole-based compounds. Liquid Crystals, 2019, 46, 131-137.	2.2	5
86	Syntheses of new diluents for medium birefringence liquid crystals materials. Liquid Crystals, 2019, 46, 700-707.	2.2	5
87	Synthesis and properties of novel 6,7-dihydrocyclopenta[5,6-b]benzofuran-based liquid crystal compounds. Liquid Crystals, 2021, 48, 190-200.	2.2	5
88	Synthesis and properties of isothiocyanate liquid crystals containing cyclohexene unit. Liquid Crystals, 2021, 48, 1392-1401.	2.2	5
89	Pervaporation Separation and Catalysis Activity of Novel Zirconium Silicaliteâ€1 Zeolite Membrane. Chinese Journal of Chemistry, 2009, 27, 1692-1696.	4.9	4
90	Improved mesophase stability of benzoxazole derivatives via dipole moment modification. Liquid Crystals, 0, , 1-11.	2.2	4

#	Article	IF	CITATIONS
91	Facile preparation of TiO2 nanocrystals inserted in monodispersed mesoporous SiO2 nanospheres for enhanced photocatalytic activity. Journal of Materials Science: Materials in Electronics, 2016, 27, 13161-13170.	2.2	4
92	New negative dielectric anisotropy liquid crystals based on benzofuran core. Liquid Crystals, 2020, 47, 2313-2322.	2.2	4
93	High birefringence nematic liquid crystals containing both thieno[3,2- <i>b</i> ]thiophene core and acetylene bond. Liquid Crystals, 2022, 49, 845-854.	2.2	4
94	Efficient Bifunctional Oxygen Electrocatalysts for Rechargeable Zinc–Air Battery: Fe 3 O 4 /Nâ^'C Nanoflowers Derived from Aromatic Polyamide. ChemCatChem, 0, , .	3.7	4
95	Synthesis and the effect of 2,3-difluoro substitution on the properties of diarylacetylene terminated by an allyloxy group. Liquid Crystals, 0, , 1-10.	2.2	3
96	Cross-linked poly(arylene ether sulfone)s with side-chain aromatic benzyltrimethyl ammonium for anion-exchange membranes. Polymer Bulletin, 2017, 74, 4329-4348.	3.3	3
97	Synthesis and properties of fluorinated terphenyl liquid crystals utilizing 5,6-dihydro-4H-cyclopenta[b]thiophene as core unit. Journal of Molecular Structure, 2022, 1267, 133612.	3.6	3
98	Oneâ€Pot Microwaveâ€Assisted Synthesis of Benzopyrano[2,3â€ <i>c</i> ]pyrazolâ€3â€one Derivatives. Journal o Heterocyclic Chemistry, 2014, 51, 1210-1214.	f <sub>2.6</sub>	2
99	Synthesis and Characterization of Mesogenic Compounds Possessing Bithiophene and Benzoxazole Units. Molecular Crystals and Liquid Crystals, 2015, 608, 25-37.	0.9	2
100	Preparation and properties of lateral monofluoro-substituted benzoxazole-based mesogenic compounds. Liquid Crystals, 0, , 1-9.	2.2	2
101	Effect of the thieno[3,4-c]pyrrole-4,6-dione on properties of the cyclic thiourea triphenylamine sensitizers. Dyes and Pigments, 2019, 161, 197-204.	3.7	2
102	Evaluation of mesomorphic and thermal stabilities for terminal epoxy liquid crystals. Journal of Molecular Liquids, 2020, 317, 113955.	4.9	2
103	Increasing the negative dielectric anisotropy of liquid crystals by fluorination of the terminal ethyl chain. Liquid Crystals, 2020, 47, 2268-2275.	2.2	2
104	New multi-fluorinated benzofuran liquid crystals with large dielectric anisotropy and improved solubility. Liquid Crystals, 2022, 49, 1753-1762.	2.2	2
105	59â€4: Fastâ€response polarization volume gratings for AR/VR displays. Digest of Technical Papers SID International Symposium, 2019, 50, 838-841.	0.3	1
106	51â€3: Highâ€birefringence Liquid Crystal for Phaseâ€only Spatial Light Modulators. Digest of Technical Papers SID International Symposium, 2018, 49, 674-677.	0.3	0
107	Organic double D–π–A sensitizers based on 2,2′-(2,2 diphenylethene-1,1-diyl)dithiophene: π-conjugation fragment effect on the photovoltaic properties. Materials Advances, 2021, 2, 6641-6646.	5.4	0